Cerebral Cortex Advance Access published August 3, 2007

Cerebral Cortex
doi:10.1093/cercor/bhm134

A Common Neural Network for Cognitive Reserve in Verbal and Object Working Memory in Young but not Old

Yaakov Stern[1,2,3], Eric Zarahn[1,3], Christian Habeck[1,2], Roee Holtzer[1,4,5], Brian C. Rakitin[1,2], Arjun Kumar[1], Joseph Flynn[1], Jason Steffener,[1,2] and Truman Brown[5]

[1]Cognitive Neuroscience Division of the Taub Institute, NY, USA, [2]Departments of Neurology and [3]Psychiatry, Columbia University College of Physicians and Surgeons, NY, USA, [4]Ferkauf Graduate School of Psychology and Department of Neurology, Albert Einstein College of Medicine, Yeshiva University, NY, USA and [5]Department of Radiology, Columbia University College of Physicians and Surgeons, NY, USA

Epidemiologic evidence suggests that cognitive reserve (CR) mitigates the effects of aging on cognitive function. The goal of this study was to see whether a common neural mechanism for CR could be demonstrated in brain imaging data acquired during the performance of 2 tasks with differing cognitive processing demands. Young and elder subjects were scanned with functional magnetic resonance imaging (fMRI) while performing a delayed item response task that used either letters (40 young, 18 old) or shapes (24 young, 21 old). Difficulty or load was manipulated by varying the number of stimuli that were presented for encoding. Load-dependent fMRI signal corresponding to each trial component (stimulus presentation, retention delay, and probe) and task (letter or shape) was regressed onto 2 putative CR variables. Canonical variates analysis was applied to the resulting maps of regression coefficients, separately for each trial component, to summarize the imaging data—CR relationships. There was a latent brain pattern noted in the stimulus presentation phase that manifested similar relationships between load-related encoding activation and CR variables across the letter and shape tasks in the young but not the elder age group. This spatial pattern could represent a general neural instantiation of CR that is affected by the aging process.

Keywords: aging, canonical variates analysis, fMRI, short-term memory

Introduction

Many studies have suggested that there is differential susceptibility to age-related memory changes and dementia that is related to variables such as education, literacy, IQ, and engagement in leisure activities (Schaie 1984; Stern et al. 1994; Gold et al. 1995; Hultsch et al. 1999; Wilson et al. 2000; Scarmeas et al. 2001; Wilson et al. 2002; Manly et al. 2003). These studies provide epidemiologic evidence for the presence of cognitive reserve (CR), where individuals with greater CR may show less severe effects of the aging process (Stern 2002). The concept of CR posits that individual differences in how tasks are processed provides differential reserve against brain pathology or age-related changes. CR might affect various cognitive tasks via a common mechanism, be mediated in a task-specific manner, or via a combination of both common and task-specific mechanisms. The goal of the current study was to see whether a common mechanism for CR across verbal and object working memory could be demonstrated in brain imaging data acquired during the performance of delayed item recognition (DIR) tasks using 2 types of stimuli.

We have hypothesized that the neural implementation of CR takes 2 forms (Stern et al. 2005). In *neural reserve*, preexisting brain networks that are more efficient or have greater capacity are less susceptible to disruption by age-related other pathology. In *neural compensation*, alternate networks compensate for pathology's disruption of preexisting networks. Both of these cases posit that the differential expression of brain networks as a function of CR may provide reserve, but in fundamentally different ways. Importantly, because the concept of neural reserve suggests that CR-related brain networks exist prior to the advent of age-related or other pathology, such networks should be expressed in young as well as older individuals.

In previous functional imaging studies we have explored the neural implementation of CR by examining the relationships between task-related activation and putative proxies for CR including IQ measures (Habeck et al. 2003, 2005; Scarmeas et al. 2003; Stern et al. 2005). However, these relationships have only been explored within single tasks. In the present study, we sought to determine whether there is a network subserving CR that was active across tests of verbal and object working memory, each of which has differing cognitive processing demands. Young and elder subjects were scanned with functional magnetic resonance imaging (fMRI) while performing one of 2 versions of a DIR task; one version used letters as the stimuli to be encoded and recognized, whereas the other used shapes that were difficult to name. In both tasks, difficulty or load was manipulated by varying the number of stimuli that were presented for encoding. Load-dependent fMRI signal corresponding to each trial component (i.e., stimulus presentation, retention delay, and probe) and task (letter or shape) was regressed onto putative CR variables. Canonical variates analysis (CVA) (Worsley et al. 1997) was applied to the resulting maps of regression coefficients, separately for each trial component, to summarize the imaging data–CR relationships. More precisely, CVA decomposes a set of original brain activation effects (e.g., relationships of brain imaging data at each voxel with a set of CR variables) into a set of latent spatial pattern/latent predictor variable pairs. The latent predictors represent the combination of the original predictors that correspond to each latent spatial pattern. We wished to determine if there were latent patterns of CR-related brain activity whose latent predictors had similar and sizeable contributions from both the letter and shape tasks. Such a pattern (which we tentatively conceive of as a network), expressed across 2 tasks with divergent processing demands, would be a likely candidate for a generic neural substrate underlying CR.

We also wished to determine whether any such CR-related spatial pattern is expressed similarly in young and old individuals. In young subjects, we have previously reported brain networks whose degree of expression correlates with CR, consistent with the concept of neural reserve. We have also described instances where the directionality of the relationship between CR and network expression differed in young and old

subjects, which is consistent with neural compensation in the older subjects (Scarmeas et al. 2003; Stern et al. 2005). In the present study, we therefore explored whether young and old individuals expressed the same CR-related network, and if so, whether the degree of expression was comparable across the 2 groups.

Materials and Methods

Subjects

Healthy young and old subjects participated in 2 separate fMRI studies using DIR tasks. Although the tasks had identical temporal structures, one used letters as the stimuli to be remembered and recognized whereas the other used shapes. Fifty-eight subjects participated in the letter task study ($N = 40$ young and 18 old); other aspects of these data have been previously reported (Habeck et al. 2005; Zarahn et al. 2005). Forty-five subjects participated in the shape task study ($N = 24$ young and 21 old).

All subjects supplied informed consent. They were screened for neurologic and psychiatric illness via a questionnaire. Elders were screened for dementia with neuropsychological testing and a functional evaluation.

The modified Mini-Mental State Examination (Stern et al. 1987), an extended version of the Folstein MMS (Folstein et al. 1975), and the Mattis Dementia Rating Scale (Mattis et al. 1976) were administered as mental status screens.

We used 2 brief measures of IQ as proxy variables for CR: the American version of the New Adult Reading test (NART) (Grober and Sliwinski 1991), and the Vocabulary subtest of the Wechsler Adult Intelligence Scale-Revised (WAIS-R) (Wechsler 1981). Both predicted IQ from the NART and age-scaled scores on the Vocabulary subtest were included in the CVA analyses described below in an effort to use an IQ measure that was generalized across the 2 tests. Because a principal component analysis showed that NART and Vocabulary were weighted equally on a common principal component, these variables were weighted equally in the image analyses described below.

Behavioral Tasks

The DIR tasks were modified from Sternberg's procedures (Sternberg 1966). Task timing and fMRI acquisition were identical across the letter and shape versions. Each DIR trial lasted a total 16 s. The sequence of events within a trial was as follows: 1) A 3-s presentation of a blank screen marked the beginning of the trial. 2) An array of either 1, 3, or 6 capital letters or 1, 2, or 3 shapes were presented for 3 s. For the letter task, the geometry of the stimuli was a 2 by 3 array, regardless of set size, with asterisks acting as nonletter placeholders for set sizes 1 and 3. For the shape task, stimuli were presented in a 1 by 3 array, with asterisks again acting as placeholders. The shapes were identical to those used in a nonverbal recognition task in previous reports (Holtzer et al. 2004; Stern et al. 2005). 3) A 7-s retention delay period, during which time the screen was blank. 4) A probe letter (lowercase) or shape, centered in the field of view, appeared for 3 s. In response to the probe, subjects indicated by a button press whether or not the probe matched an item in the study array (right index finger button press to indicate "yes," left index finger button press to indicate "no"). Subjects were instructed to respond as accurately as possible. No feedback about their performance was given during the scanning session.

Each experimental block contained 10 trials at each of the 3 set sizes, with 5 true negative and 5 true positive probes per set size. The presentation of trials of different set sizes was pseudorandomly sequenced via a random-without-replacement scheme. Blank trials (presentation of a blank screen for 2 s, requiring no behavioral output) were pseudorandomly interspersed between DIR trials to both provide a baseline condition for positive control purposes and reduce the likelihood of neurophysiological responses predictive of the beginning of trials. The pseudorandomization of these blank trials was via a random-without-replacement scheme (thus, more than one blank trial could occur sequentially, leading to an effectively jittered intertrial interval), with a total of 70 blank trials per block. The duration of each block was 620 s. There were approximate 1-min breaks between blocks. Prior to the acquisition of fMRI data, subjects were trained on 7 blocks of DIR trials, the first 6 of which were administered with feedback.

Blood oxygen level–dependent (BOLD) fMRI data were acquired for 3 experimental blocks per subject, yielding a total of 30 experimental trials per set size per subject.

fMRI Data Acquisition

During the performance of each block of each DIR task, 207 T_2*-weighted images, which are BOLD images (Kwong et al. 1992; Ogawa et al. 1993), were acquired with an Intera 1.5-T Phillips MR scanner equipped with a standard quadrature head coil, using a gradient echo echo-planar (GE-EPI) sequence (time echo/time repetition [TE/TR] = 50 ms/3000 ms; flip angle = 90°; 64 × 64 matrix, in-plane voxel size = 3.124 mm × 3.124 mm; slice thickness = 8 mm [no gap]; 17 trans-axial slices per volume). Four additional GE-EPI excitations were performed before the task began, at the beginning of each run, to allow transverse magnetization immediately after radio-frequency excitation to approach its steady-state value; the image data for these excitations were discarded. A T_2-weighted, fast spin echo image was also acquired from each subject for spatial normalization purposes (TE/TR = 100 ms/2000 ms; flip angle = 90°, 256 × 256 matrix; in-plane voxel size = 0.781 mm × 0.781 mm; slice thickness = 8 mm [no gap]; 17 trans-axial slices per volume).

Task stimuli were back-projected onto a screen located at the foot of the MRI bed using an LCD projector. Subjects viewed the screen via a mirror system located in the head coil. Responses were made on an LUMItouch response system (Photon Control Company). Task onset was electronically synchronized with the MRI acquisition computer. Task administration and data collection (RT and accuracy) were controlled using PsyScope (Cohen et al. 1993).

Behavioral Data Analysis

Discriminability (dL) (Snodgrass and Corwin 1998) and median reaction time (RT) were assessed for effects of set size, group, and group × set size interaction via repeated measures General Linear Model (GLM). For each subject, linear regression analysis was used to calculate the slope of RT across set size, the RT intercept (i.e., imputed value at set size = 0), and the slope of dL.

fMRI Statistical Analysis

All image preprocessing and analysis were implemented using the SPM99 program (Wellcome Department of Cognitive Neurology) and other code written in MATLAB 5.3 (Mathworks, Natick, MA). The following steps were taken in turn for each subject's GE-EPI data set: data were temporally shifted to correct for the order of slice acquisition, using the first slice acquired in the TR as the reference. All GE-EPI images were realigned to the first volume of the first session. The T_2-weighted (structural) image was then coregistered to the first EPI volume using the mutual information coregistration algorithm implemented in SPM99. This coregistered high-resolution image was then used to determine parameters (7 × 8 × 7 nonlinear basis functions) for transformation into a Talairach standard space (Talairach 1988) defined by the Montreal Neurologic Institute template brain supplied with SPM99. This transformation was then applied to the GE-EPI data, which were resliced using sinc-interpolation to 2 mm × 2 mm × 2 mm.

The fMRI data analysis comprised 2 levels of voxel-wise GLMs (Holmes and Friston 1998): the first-level GLM is a time-series analysis that yields summary measures to be used in the second-level GLM, which affords statistical inference at the population level. In the (subject-separable) first-level GLM, the GE-EPI time series were modeled with regressors representing the expected BOLD fMRI response (implicitly, relative to the blank intervals) to the 3 DIR trial components of memory set presentation, retention delay, and probe presentation/response, separately for each crossing of the set size and true positive/true negative factors. The regressors were constructed by convolutions of an indicator sequence (i.e., a train of discrete-time delta functions) representing DIR trial component onsets, an assumed BOLD impulse response function (as represented by default in SPM99), and a rectangular function of duration dictated by the duration of the assumed neural response (Zarahn 2000). As with most event-related designs, the current task design is results in colinearity across the regressors used for

each task phase. Colinearity weakens estimability, impairing to some degree the ability to detect task-related signal change that is unique to each task phase. The analytic approach employed in the first-level GLM was intended to reduce colinearity as much as possible, and was derived based on prior knowledge and regression diagnostics. These diagnostic indicated that the modeling of each phase was acceptable, with minimal "bleed" across trial components. Based on these considerations, 2 rectangular functions (and hence, 2 regressors) were used for the trial component of memory set presentation: one modeling a relatively brief (400 ms) neural response at the beginning of that trial component, and another modeling a neural response lasting throughout that entire component (3000 ms); the same 2 rectangular functions were used for probe presentation. A single rectangular function of 7000-ms duration was used for the retention delay. For both the memory set presentation and probe presentation trial components, a linear combination (i.e., a contrast) of the 2 parameter estimates was computed which estimated the area under the curve of the neural response for that trial component. For the retention delay trial component, the analogous contrast was simply the coefficient of its single basis function. More details about the design of the first level GLM analysis are available in the supplementary material. Linear combinations (i.e., contrasts) of the estimated coefficients of these predictors were computed to yield estimates of the linear effect with respect to set size of the area under the curve of the neural response for each trial component in each subject. The contrast estimate images were then intensity normalized via voxel-wise division by the time-series mean and spatially smoothed with an isotropic Gaussian kernel (full-width-at-half-maximum = 8 mm). The resulting images (3 trial components = 3 images/subject) were used as the dependent variables in a second-level GLM.

In the second-level GLM, the predictors, separable by age group (young and elder) and task (letter and shape) were NART IQ and WAIS-R Vocabulary age-scaled score (i.e., 2 proxy variables for CR), RT slope, RT intercept, and a constant term. Multidimensional contrasts (e.g., like those used to specify *F*-tests) were constructed separately for each of the 3 trial component (stimulus, retention, and probe). Each of these multidimensional contrasts comprised the coefficients of the 2 CR variables for the 2 age groups and the 2 tasks (letter and shape). Thus, there were 4 contrasts for each of the 3 trial components. As explained above, the scores on the 2 CR measures were weighted equally in each contrast. For each trial component, the number of latent spatial patterns needed to summarize the brain images corresponding to the 4 contrasts was assessed statistically using sequential latent root testing in the context of CVA (Worsley et al. 1997). Details of this method can be found elsewhere (Zarahn et al. 2005).

The predicted expression of the any latent spatial pattern over dependent variable index is called its latent predictor. As in standard CVA/factor analysis of behavioral measures, each latent predictor is necessarily a linear combination of the original predictors of the GLM. In this case, these original predictors consist of the 2 CR proxy scores (NART and Vocabulary scores) used to model imaging data separately for the 2 tasks and age groups (and so 4 original predictors per multidimensional contrast). For each identified significant latent spatial pattern, we present the weights of the linear combination of original predictors that yield the corresponding latent predictor. Because the 2 CR variables were equally weighted in the analyses, their weights in the latent spatial pattern are equivalent. For simplicity, we therefore present a single CR variable, which representing equal weighting of each of scores on the 2 measures.

The latent predictor weights for each significant latent spatial pattern were examined to see if the weights were significantly different from zero and were similar across task types. Post hoc analyses also compared the latent predictor weights across contrasts of interest.

We were particularly interested in determining if there was a pattern that was expressed similarly in both the letter and shape task. We had no a priori assumptions about the task phase in which such a pattern would be present, or whether that pattern would be expressed similarly or differentially as a function of age.

We present the topography of latent spatial patterns (scaled by their corresponding singular values) thresholded for descriptive purposes (i.e., for all tables and figures) at a t value corresponding to $P < 0.001$ uncorrected for multiple comparisons and a cluster size of 50 voxels. This threshold is more lenient than that required for map-wise statistical significance with $\alpha = 0.05$, either without (Worsley 1994) or with (Friston et al. 1996) cluster size correction, and so is only meant to provide a somewhat condensed description of the significant spatial patterns. Likely cytoarchitectonic labels for cluster maxima in these thresholded patterns were obtained using Talairach daemon (Lancaster et al. 2000).

Results

Demographics

Subject demographics and scores on the CR proxies, NART IQ and WAIS-R Vocabulary age-scaled score, for the subjects in the 2 studies (letters and shape task) are summarized in Table 1. For subjects in the letter task study, education was comparable in the young and old subjects, but both NART IQ and Vocabulary scores were slightly but significantly lower in the older group. In the shape task, education, NART IQ, and Vocabulary performance were comparable across the young and old subjects.

DIR Task Performance

Letter Task

Median RT and dL for each set size are summarized in Table 2.

There was a main effect of group on RT ($F_{1,56} = 8.4$, $P = 0.005$), indicating an overall slowed RT in elders compared with young subjects averaged across set sizes. The interaction of age group and set size was significant ($F_{1.7,96.1} = 6.1$, $P = 0.005$). The RT slope was significantly larger in the elders 85.7 (35.7) ms per letter than in the young (59.0 [30.8] ms per letter; $t(56) = -2.91$, 2-tailed $P = 0.005$).

There was a main effect of group on accuracy (dL; $F_{1,56} = 9.3$, $P = 0.003$). There was a significant set size effect ($F_{1.8,101.6} = 5.8$ $P < 0.008$) and the interaction of group and set size were borderline ($F_{1.8,101.6} = 2.9$, $P = 0.062$). Inspection of the means suggests a stronger effect of set size on accuracy in the old subjects. However, accuracy remained quite good in both groups.

Shape Task

Median RT and dL for each set size are summarized in Table 2.

There was a main effect of group on RT ($F_{1,43} = 11.9$, $P < 0.001$), indicating an overall slowed RT in elders compared with young subjects averaged across set sizes. The interaction of age group and set size was significant ($F_{1.8,78.5} = 8.4$, $P = 0.001$). The RT slope was significantly larger in the elders 199.8 (95.8) ms per shape than in the young 124.4 (64.2) ms per shape; $t(43) = -3.14$, 2-tailed $P = 0.003$).

There was also a main effect of group on accuracy ($F_{1,43} = 4.5$, $P = 0.04$). The accuracy of both young subjects and elder

Table 1
Demographics and performance on CR proxy tests of subjects in the 2 studies: letter and shape DIR

Subject demographics	Letter task		Shape task	
	Young ($N = 40$)	Old ($N = 18$)	Young ($N = 24$)	Old ($N = 21$)
Age	25.1 (3.9)	74.4 (6.9)*	24.0 (3.9)	75.8 (5.1)*
Education	15.7 (1.4)	15.3 (2.4)	14.7 (2.2)	15.8 (3.1)
Gender	30 M/10 F	7 M/11 F	12 M/12 F	11 M/10 F
NART IQ	120.3 (6.1)	116.8 (6.4)*	114.9 (6.6)	118.3 (6.5)
WAIS-R vocabulary (AgSc)	14.5 (2.8)	12.4 (1.9)*	13.0 (3.6)	14.5 (2.8)

*Old young comparison, $P < 0.05$.

subjects decreased with set size ($F_{2,84.6}$ = 118.5 P < 0.001); the interaction of group and set size was not significant ($F_{2,84.6}$ = 1.0, nonsignificant [ns]).

Canonical Variates Analysis

Table 3 summarizes the sequential latent root test results across the 3 trial components. In the stimulus presentation phase, sequential root testing in the CVA analysis detected 2 latent spatial patterns. In 2 other phases, only one significant latent spatial pattern was identified. Figures 1–4 present bar graphs of the latent predictor variable weights associated with each of the identified latent spatial patterns as well as surface renderings of each patterns. Local maxima for each pattern are listed in Table 4. The bar graphs of the latent predictor variable weights demonstrate that the first latent spatial patterns noted in all 3 trial phases (Figs 1, 3, and 4) are associated primarily with the letter task. In each case there is a strong negative association with elders' CR scores. In addition, during the stimulus phase there is a positive association with the CR scores in the young subjects. Pattern expression differed significantly from 0 in all cases.

In contrast, the second latent spatial pattern detected during the stimulus phase (Fig. 2) was expressed in both the letter and the shape task. In the young subjects, pattern expression was negatively related to the CR scores in both the letter and shape tasks. This indicates that brain areas with negative weights showed increased load-related expression with increasing levels of CR. For example, with increasing CR there was increased expression in right and left superior frontal gyrus and concomitant reduced expression in left medial frontal gyrus. Subsequent testing revealed that pattern expression was significant in both tasks in the young subjects (for the letter task, t = 3.390, P < 0.001; for the shape task, t = 5.941, P < 0.001). A post hoc test revealed that young subjects' CR-related expression of this pattern was over 10 times greater in the shape than in the letter task ($t(62)$ = 7.2, P < 0.0001). In the elder subjects, the letter task was also negatively related to the CR scores, but the shape task was positively related to the CR scores. Elders' expression of this pattern did not differ significantly from 0 in either the letter (t = 1.075, ns) or the for the shape task (t = 1.267, ns).

Table 2
Performance on the shape and letter DIR tasks

Letter task					Shape task				
# Letters	Young		Old		# Shapes	Young		Old	
	Mean	SD	Mean	SD		Mean	SD	Mean	SD
Median RT									
1	846.7	170.5	893.5	152.6	1	1063.2	196.1	1134.1	149.9
3	1015.3	202.7	1076.7	211.6	2	1221.1	212.2	1450.2	147.9
6	1148.2	227.3	1325.4	293.2	3	1311.9	184.9	1533.8	221.4
Mean DL									
1	6.2	0.9	5.8	1.0	1	5.3	1.8	4.5	1.4
3	6.0	1.2	5.5	1.2	2	3.5	1.9	2.5	1.2
6	6.0	0.9	4.7	2.1	3	1.7	1.0	1.3	0.7

Table 3
Sequential latent root testing results for contrasts relating load-dependent processing to CR variables in each of the 3 task phases

	Test for at least 1 component		Test for 2 components		Test for 3 components		Inferred number of patterns at $\alpha = 0.05$
	$F_{1342,36\ 091}$	P	$F_{1007,32\ 498}$	P	$F_{671,27\ 109}$	P	
Stimulus	2.02	<0.0001	1.09	0.02	0.93	0.89	2
Retention	1.39	<0.0001	1.03	0.22	N/A	N/A	1
Probe	1.22	<0.0001	0.95	0.84	N/A	N/A	1

Note: N/A, not applicable.

Discussion

We examined the relationship between CR and load-related activation during the performance of 2 types of DIR tasks, one using verbal stimuli (letters) and the other using objects (nonsense shapes). Latent patterns whose expression was related to the CR scores were identified during each phase (stimulus presentation, retention delay and probe) of the DIR tasks. In each phase, a CR-related pattern was identified that was expressed only during performance of the letter task. During the stimulus presentation phase such a pattern was expressed by both young and old subjects but the directionality of the relationship with the CR measures differed in the 2 groups. In the retention and probe phases such patterns were expressed only by the older subjects. Of more interest to the intent of this current report, in the young group a second spatial pattern was identified in the stimulus presentation phase that manifested similar relationships between CR and load-related activation across both the letter and shape DIR tasks. In the elder group, expression of this pattern as a function of CR differed in directionality across the 2 tasks, and the magnitude of pattern expression did not reach significance.

The analyses in this paper focused on identifying spatial patterns of activation that systematically differ as a function of CR. The derived spatial patterns therefore have no relationship with the neural networks associated with the specific demands of the stimulus presentation, retention delay, or probe phases of these 2 types of DIR tasks. Although it is not the subject of the current report, separate analyses demonstrate that the stimulus presentation phase activated different brain areas in the letter and shape task (data not shown). This would be expected given the divergent demands associated with processing verbal and nonverbal stimuli.

Similarly, the analysis does not concern itself with whether differential expression a CR-related spatial pattern is associated with better or worse performance. In fact, we explicitly eliminated the possibility of such a relationship. In the CVA analyses, the design matrix included the slope and intercept of RT on set size as predictors of no interest. Thus, any detected relationships of neural activity with CR variables could not be mediated by these RT variables. This reduces the chance that CR-related network expression is influenced by differences in performance across individuals. We relied on the effortful processing in these tasks (by looking at load-related activation) to elicit CR-related networks, independent of performance. This means that a high-CR young person, although badly performing in a high-demand task, will still show a pure instantiation of the CR network. The inference that we wish to draw is that these network might represent the neural instantiation of CR, or alternately that the ability to invoke these network might underlie the benefits that CR imparts.

Despite the divergent demands associated with processing verbal and nonverbal stimuli, in the young subjects there was a brain activation pattern during stimulus presentation whose expression bore a similar relationship to CR variables in both

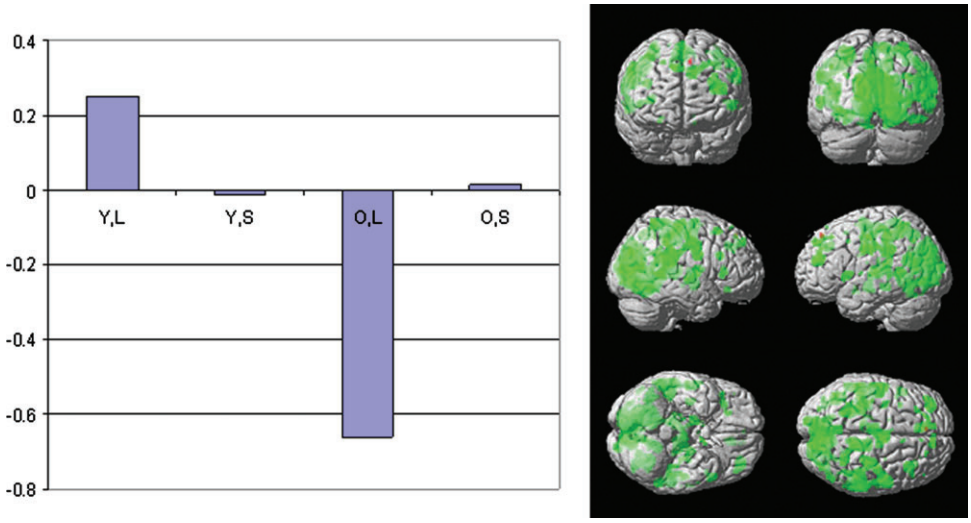

Figure 1. For the first significant spatial pattern identified by sequential latent root testing during the encoding phase, a plot of the latent predictor weights for each of the independent variables in the model is presented. Codes for the variables are Y = young; E = Elder; L = letter; S = shape. The surface rendering of the positively (red) and negatively (green) weighted aspects of the spatial pattern is also presented. Each latent spatial pattern is scaled by its corresponding singular value and thresholded at a *t* value corresponding to $P < 0.001$ uncorrected for multiple comparisons and a cluster size of 50 voxels. The negative latent predictor weight in the elders for the letter task indicates that the negatively weighted aspects of the pattern were expressed to a greater degree in elders with higher measured CR, with concomitant lowered expression of the positively weighted aspects. In contrast, during letter task performance the positively weighted aspects were expressed to a greater degree by younger subjects with higher CR.

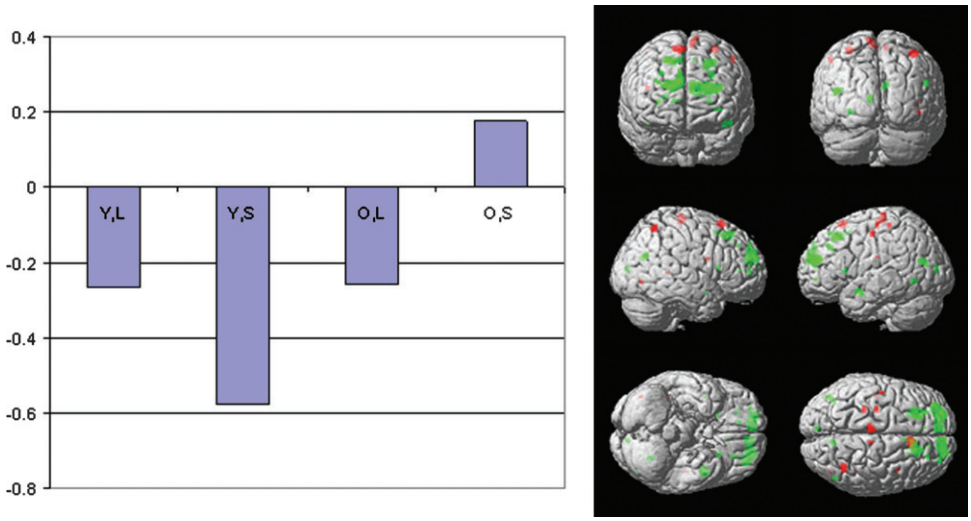

Figure 2. The plot of the latent predictor weights for each of the independent variables in the model and surface rendering for the second significant spatial pattern identified by sequential latent root testing during the encoding phase. See Figure 1 for details of labeling and color conventions. In the young subjects, this pattern was expressed in both the letter and the shape task. Pattern expression was negatively related to the CR scores in both the letter and shape tasks. This indicates that brain areas with negative weights showed increased expression with increasing levels of CR. Similar directionality of pattern expression was noted for the elders during performance of the letter but not the shape task, and the degree of pattern expression did not reach significance in the elders.

tasks. This CR network may therefore represent a more generalized process that is not task specific and that is expressed during younger subjects' performance of a wide range of cognitive tasks. This spatial pattern could therefore represent a generalized neural instantiation of CR. Because this pattern reflects a CR-related network that is used by healthy individuals it meets our previously proposed criteria for neural reserve (Stern et al. 2005). We have proposed neural reserve as a possible neural implementation of CR in which differential expression across individuals of preexisting brain networks might render some less susceptible than others to disruption by age-related other pathology. Some aspects of CR should be mediated by individual variability in network expression that is already present in healthy individuals.

Although the young subjects expressed this pattern as a function of CR during both the letter and shape tasks, pattern expression was significantly greater during the shape task. As is evident from the behavioral data in Table 2, the shape version of the DIR task was much more demanding, yielding both longer RT and poorer discriminability. These differences reflect the fact that letters are well learned stimuli which should be encoded almost automatically, whereas the shape stimuli were complex and unfamiliar. The increased expression of the CR-related pattern associated with load-related encoding of the

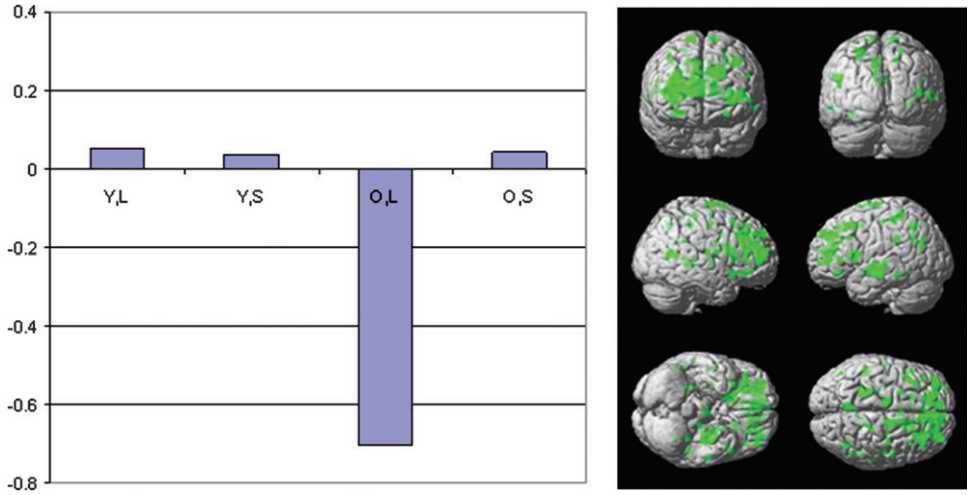

Figure 3. The plot of the latent predictor weights for each of the independent variables in the model and surface rendering for the significant spatial pattern identified by sequential latent root testing during the retention phase. See Figure 1 for details of labeling and color conventions. The negative latent predictor weight in the elders for the letter task indicates that the negatively weighted aspects of the pattern were expressed to a greater degree in elders with higher measured CR, with concomitant lowered expression of the positively weighted aspects. This pattern was not expressed by the young subjects.

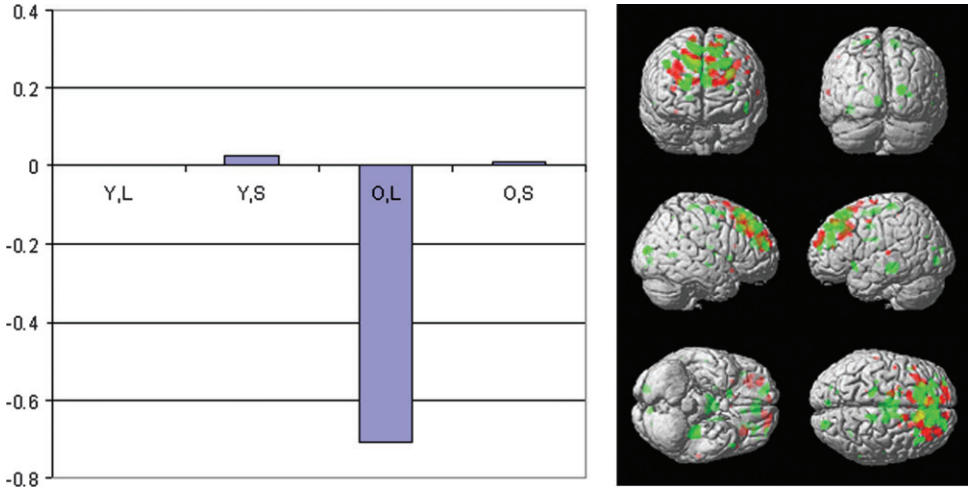

Figure 4. The plot of the latent predictor weights for each of the independent variables in the model and surface rendering for the significant spatial pattern identified by sequential latent root testing during the probe phase. See Figure 1 for details of labeling and color conventions. The negative latent predictor weight in the elders for the letter task indicates that the negatively weighted aspects of the pattern were expressed to a greater degree in elders with higher measured CR, with concomitant lowered expression of the positively weighted aspects. This pattern was not expressed by the young subjects.

shape stimuli might therefore reflect the fact that the cognitive processes mediated by this set of brain areas are engaged to a greater degree in this more demanding situation.

It should be stressed that the graphed weights of the expression of this common pattern are for the relationship between CR and expression of this spatial pattern. That is, this pattern is expressed to a greater degree per unit of the CR measures in the shape task than in the letter task. This relationship has no direct link to overall levels of task-related activation (i.e., as a function of task difficulty). It is not the case that the more demanding nature of the shape DIR task leads to greater overall levels of fMRI activation, and that this in turn is reflected in greater regression coefficients between fMRI activation and CR. In mathematical terms, if such a greater level of activation were additive, then it would manifest in the *y*-intercept of the regression model, not the CR coefficient. For similar reasons, it also would not be correct to conclude that individuals with higher measured CR *need to* recruit this network to a greater degree than those with lower CR in order to perform the tasks. Rather, we hypothesize that the relatively increased expression of the CR-related pattern during encoding of the shape stimuli might reflect the fact that the cognitive processes mediated by this set of brain areas are engaged to a greater degree in this more demanding situation.

The older subjects' expression of this pattern did not reach significance. This may be due to more limited power to detect a relationship between CR and pattern expression in this smaller group ($N = 18$ for elders vs. 40 for the young subjects). Still, it is of interest to note that in the elders pattern expression was not consistent across the 2 tasks. Notably, the directionality of pattern expression was similar to that in the young subjects for the letter but not the shape task. Follow-up studies are

Table 4

Local maxima for the CR-related spatial patterns expressed during DIR task performance. $P < 0.05$ and extent threshold of 50 voxels was applied to all results

First spatial pattern noted during encoding phase

	t-value	Talairach coordinates	Location		BA
Positive weights	No significant areas				
Negative weights	7.15	−6 −87 1	Left	Lingual gyrus	17
	6.34	−32 −62 −5	Left	Fusiform gyrus	19
	5.95	2 −72 28	Right	Precuneus	31
	5.99	46 −34 22	Right	Insula	13
	5.71	59 −30 22	Right	Inferior parietal lobule	40
	5.47	55 −2 37	Right	Precentral gyrus	6
	5.64	12 −25 42	Right	Cingulate gyrus	31
	4.90	10 −38 59	Right	Paracentral lobule	5
	4.43	30 −47 61	Right	Superior parietal lobule	7
	5.08	−10 36 29	Left	Medial Frontal Gyrus	9
	4.76	−12 46 33	Left	Superior Frontal Gyrus	9
	4.04	−20 43 38	Left	Superior frontal gyrus	9
	5.00	−36 48 18	Left	Middle frontal gyrus	10
	4.53	−30 44 22	Left	Middle frontal gyrus	10
	4.78	−8 −15 47	Left	Medial frontal gyrus	6
	4.38	4 −3 55	Right	Medial frontal gyrus	6
	4.03	12 −9 47	Right	Cingulate gyrus	31
	4.77	−50 14 1	Left	Inferior frontal gyrus	
	4.69	−57 −8 32	Left	Precentral gyrus	4
	4.68	−26 −44 48	Left	Precuneus	7
	4.38	−51 −33 29	Left	Inferior parietal lobule	40
	4.47	−55 −46 6	Left	Middle temporal gyrus	21
	4.31	16 −8 −6	Right	Medial globus pallidus	
	4.28	−14 −57 -14	Left	Declive	
	4.25	−38 −61 18	Left	Middle temporal gyrus	39
	3.39	−44 −50 19	Left	Superior temporal gyrus	39
	3.33	−46 −55 27	Left	Superior temporal gyrus	39
	4.19	−6 −60 47	Left	Precuneus	7
	4.16	36 −12 2	Right	Claustrum	
	4.16	−18 −12 −6	Left	Medial globus pallidus	
	4.09	−26 −17 8	Left	Putamen	
	3.88	−30 −14 1	Left	Putamen	
	4.10	2 50 36	Right	Medial frontal gyrus	9
	4.06	55 −16 −3	Right	Superior temporal gyrus	21
	3.78	53 −6 2	Right	Superior temporal gyrus	22
	3.75	59 −4 8	Right	Superior temporal gyrus	22
	3.80	38 22 21	Right	Frontal lobe, subgyral	
	3.74	46 23 1	Right	Inferior frontal gyrus	
	3.71	34 26 6	Right	Inferior frontal gyrus	45
	3.58	−46 −11 43	Left	Precentral gyrus	4

Second spatial pattern noted during encoding phase

	t-value	Talairach coordinates	Location		BA
Positive weights	4.97	8 22 56	Right	Superior frontal gyrus	6
	3.80	−6 −20 64	Left	Medial frontal gyrus	6
Negative weights	7.69	14 57 21	Right	Superior frontal gyrus	10
	7.04	−32 50 20	Left	Superior frontal gyrus	10
	5.74	−8 53 18	Left	Medial frontal gyrus	9
	3.70	−16 57 19	Left	Superior frontal gyrus	10
	4.36	14 26 45	Right	Medial frontal gyrus	8
	3.49	6 16 47	Right	Medial frontal gyrus	6
	4.08	−22 27 41	Left	Middle frontal gyrus	8

Spatial pattern noted during retention phase

	t-value	Talairach coordinates	Location		BA
Positive weights	No significant areas				
Negative Weights	5.38	22 45 14	Right	Medial frontal gyrus	9
	4.96	14 53 8	Right	Medial frontal gyrus	10
	4.69	30 53 8	Right	Middle frontal gyrus	10
	4.92	−30 −14 −1	Left	Putamen	
	4.72	−34 −18 −8	Left	Caudate tail	
	4.25	−26 −8 −6	Left	Putamen	
	4.69	−8 52 31	Left	Superior frontal gyrus	9
	4.46	−14 38 13	Left	Anterior cingulate	32
	4.15	−20 44 29	Left	Superior frontal gyrus	9
	4.52	12 −6 68	Right	Superior frontal gyrus	6
	4.47	16 18 16	Right	Caudate	
	3.65	22 20 6	Right	Putamen	
	4.35	−40 20 43	Left	Middle frontal gyrus	8
	4.25	40 −58 14	Right	Middle temporal gyrus	19
	4.17	−8 −54 45	Left	Precuneus	7

continued

Table 4

continued

Spatial pattern noted during retention phase

	t-value	Talairach coordinates	Location		BA
	3.44	−8 −55 30	Left	Cingulate gyrus	31
	4.07	8 33 39	Right	Medial frontal gyrus	8
	3.50	12 33 30	Right	Cingulate gyrus	32
	4.00	−24 −31 49	Left	Postcentral gyrus	3
	3.93	−22 −38 55	Left	Subgyral	40
	3.97	28 36 −9	Right	Middle frontal gyrus	47
	3.87	22 29 −12	Right	Middle frontal gyrus	11
	3.82	−30 45 0	Left	Subgyral	
	3.74	−42 45 9	Left	Middle frontal gyrus	46
	3.53	−32 56 −3	Left	Superior frontal gyrus	10
	3.80	−50 −35 29	Left	Inferior parietal lobule	40

Spatial pattern noted during probe phase

	t-value	Talairach coordinates	Location		BA
Positive weights	7.62	−10 56 27	Left	Superior frontal gyrus	9
	7.51	10 29 41	Right	Medial frontal gyrus	8
	3.54	22 18 47	Right	Superior frontal gyrus	8
	6.33	30 37 33	Right	Middle frontal gyrus	9
	4.19	38 38 28	Right	Superior frontal gyrus	9
	6.22	−8 39 39	Left	Medial frontal gyrus	8
	6.15	−30 30 26	Left	Middle frontal gyrus	9
	5.03	−36 25 36	Left	Precentral gyrus	9
	5.92	−14 63 13	Left	Superior frontal gyrus	10
	5.62	−22 59 17	Left	Superior frontal gyrus	10
	5.88	−16 18 58	Left	Superior frontal gyrus	6
	4.51	−8 20 58	Left	Superior frontal gyrus	6
	4.78	28 50 20	Right	Middle frontal gyrus	10
Negative weights	7.74	−26 35 37	Left	Middle frontal gyrus	8
	5.59	−12 48 34	Left	Superior frontal gyrus	8
	7.46	8 46 33	Right	Superior frontal gyrus	9
	7.17	14 41 35	Right	Superior frontal gyrus	9
	7.04	−2 44 18	Left	Medial frontal gyrus	9
	7.35	−28 46 23	Left	Superior frontal gyrus	10
	7.31	8 36 50	Right	Superior frontal gyrus	8
	7.30	−14 30 46	Left	Superior frontal gyrus	8
	5.16	14 24 54	Right	Superior frontal gyrus	6
	6.95	20 55 10	Right	Superior frontal gyrus	10
	4.82	16 51 18	Right	Superior frontal gyrus	9
	5.76	−36 −28 −7	Left	Caudate tail	
	4.49	−2 −2 37	Left	Cingulate gyrus	24
	4.30	20 −85 15	Right	Middle occipital gyrus	18
	4.25	10 −7 56	Right	Medial frontal gyrus	6
	3.78	12 6 51	Right	Medial frontal gyrus	6
	3.92	−6 −7 56	Left	Medial frontal gyrus	6
	3.87	−4 −15 17	Left	Thalamus	
	3.87	6 −11 17	Right	Thalamus	

Note: The spatial patterns are illustrated in Figure 2.

needed to test the idea that the CR-related pattern can be used by elders in the simpler letter task, but not in the more challenging shape task. It is also intriguing to speculate that the reversal of the directionality of expression of the spatial pattern by the elders during the shape task may represent a reorganization of this set of brain areas with aging.

Separate CR-related spatial patterns were also noted in each task phase that were particular to the letter task. During the stimulus phase this pattern was present in both young and old subjects, although expressed in opposite directions. In the retention and probe phases, the pattern was expressed only by the older subjects. Identification of these patterns suggests that aspects of CR-related processing may be task specific, and that these may coexist with more generalized aspects of CR. Because the CR-related pattern noted during stimulus presentation was expressed differentially by young and old subjects it may represent a reorganization of this set of brain areas in compensation for the disruption of this network brought on by aging. During the retention and probe phases of the task, the

CR-related patterns were expressed only by the elder subjects. These spatial patterns may also represent networks used by the elders to compensate for disruption of the preexisting networks typically used by younger individuals. We have previously suggested that both types of changes—reorganization of previously used networks or utilization of new networks—be labeled neural compensation.

The approach employed here to investigate the neural correlates underlying CR rests on the assumption that there is differential load-related activation as a function of CR. Load-related aspects of activation theoretically represent a purer measure of brain function than a simple average across set sizes, or activation at any one set size. The parametric modulation obviates the pure insertion assumption of task/control subtractions. Also, we have hypothesized that differential processing as a function of CR can best be seen in situations where task load is systematically manipulated because CR might be more related to the coping with increases in task demand than to task-specific features. In the case of neural reserve, differential response of a brain network across individuals as task load increases can be an index of the efficiency or capacity of the system.

As the goal of this study was to assess the latent structure of relationships between brain activation and CR, we used CVA. This type of question could not be addressed with statistical parametric mapping, which can be used to test for the existence of effects at locations in the brain, but not to determine their latent structure (i.e., how similar different effects are across the brain).

It is notable that the common CR-related spatial pattern was found not only across 2 different tasks, but also across 2 separate groups of young subjects. This adds additional weight to the idea that this pattern is a generalized neural expression of CR. The use of different samples in the type of CVA performed is valid when the assumed covariance matrix for the fMRI data is correct, which implies structure appropriate to accommodate repeated measures covariance as well as between subjects variance. The covariance matrix we used modeled these components accordingly.

Previous work suggests that Vocabulary scores and NART IQ are each proxies for CR. We therefore included both of these measures in the current analysis. The correlation between the 2 variables was very high ($r = 0.72$ in all; 0.74 in young, and 0.72 in old subjects), prompting us to weight them equally in each contrast. This approach effectively investigated the relationship between the common expression of these 2 CR variables and load-related activation. Using these measures of IQ as proxies for CR raises some important theoretical issues. We do not feel that IQ is synonymous with CR; it is one convenient measure. Epidemiologic data suggest a set of factors make separate and independent contributions to CR, including IQ, educational, and occupational attainment, and engaging in leisure activities (e.g., Richards and Sacker, 2003). Still, these studies suggest that all of these CR proxies are associated with reduced risk of incident dementia and slower age-related cognitive decline. It could be argued that our present results relate more to IQ than to CR in general, because only IQ measures were used as covariates. However, because these IQ measures have been used as one measure of CR, and have yielded similar findings as other CR measures in epidemiologic studies, we discuss these findings in the context of CR. We used only IQ measures in this analysis because some of the other CR proxies are not as relevant to younger subjects. Many of them are still in school so total educational attainment is not yet established. Similarly, occupational attainment and later life leisure activities are not yet relevant. Still, it will be important to see how expression of the networks described here relates to other measures of CR. For example, both IQ measures that were used are verbally weighted and it would be useful to extend the assessment to nonverbal IQ measures. Further research will allow us to understand whether different influences on CR (IQ, education, occupation, etc.) make similar or separable contributions to the neural networks which underlie this construct.

In previous reports, using a continuous nonverbal recognition task, we noted age differences in the pattern of task-related activation that was associated with CR (Scarmeas et al. 2003; Stern et al. 2003, 2005). We argued that these differences were compatible with the concept of neural compensation: the elders were using different brain networks than the younger subjects in order to compensate for age-related neural changes. We have not previously addressed potential old/young differences in CR during performance of these 2 versions of the DIR task. The current results again suggest that for the most part CR-related pattern expression differs in the young and old. These results are consistent with the neural compensation model.

Functional interpretation of the brain areas implicated in the general CR network expressed by the younger subjects must be tempered by the consideration that the relation of CR is to the expression of the entire spatial pattern. Thus, any area included in the pattern is mainly of interest in relation to all of the other areas in that pattern. This makes it difficult to reference the observed pattern to brain areas that have been associated with specific tasks in voxel-based analyses. Still, many of the areas included in the pattern here have been noted in studies of control processes such as task switching (Braver et al. 2003; Wager et al. 2003), as well as in some studies of working memory (Wager and Smith 2006). In a previous fMRI study using a continuous recognition task for nonverbal stimuli (Stern et al. 2003), we found several of the same areas noted here were differentially activated as a function of CR during both the encoding and retrieval phases of the task. As in the current study, increased expression of these areas was associated with higher measured CR. These consistent findings across studies and tasks provide a preliminary suggestion that control processes may be an important component of some aspects of CR.

This study raises 2 important sets of questions that must be addressed in future studies. First, it will be of interest to see if expression of this CR-related network by younger subjects can be detected during the performance of tasks not used in the current study. If the network is expressed across multiple tasks it would support the idea that it mediates a general feature of CR.

Perhaps more important is to determine whether differential expression of this pattern actually imparts reserve against the neural effects of aging. One way to address this question would be to measure expression of this network in a set of younger subjects and then follow them over time, with the prediction that higher expression will predict slower progression of age-related cognitive changes. An alternate approach is to develop measures of age-related pathology. Higher expression should then able to counteract the effects of age-related pathology. Concretely, this means that in a regression model, network expression and any measure of such pathology should have *oppositely* signed weights when trying to account for the clinical presentation of disease and neuropsychological performance.

In summary, in young but not old subjects a spatial pattern or brain network was noted whose expression as task load increases correlates with measures of CR during performance of a verbal and a object working memory task. This network therefore appears to represent a nontask specific neural instantiation of CR, more specifically of neural reserve.

Supplementary Material

Supplementary material can be found at http://www.oxfordjournals.org/.

Funding

National Institute on Aging grant RO1 AG26158.

Notes

Conflict of Interest: None declared.

Address correspondence to Yaakov Stern, Taub Institute, 630 W 168th Street, New York, NY 10032. Email: ys11@columbia.edu.

References

Braver TS, Reynolds JR, Donaldson DI. 2003. Neural mechanisms of transients and sustained cognitive control during task switching. Neuron. 39:713–726.

Cohen J, MacWhinney B, Flatt M, Provost J. 1993. PsyScope: a new graphic interactive environment for designing psychology experiments. Behav Res Methods Instr Comput. 25:257–271.

Folstein MF, Folstein SE, McHugh PR. 1975. 'Mini-mental state': a practical method for grading the cognitive state of patients for the clinician. J Psychiatr Res. 12:189–198.

Friston KJ, Holmes A, Poline J-B, Price CJ, Frith CD. 1996. Detecting activations in PET and fMRI: levels of inference and power. Neuroimage. 4:223–235.

Gold DP, Andres D, Etezadi J, Arbuckle T, Schwartzman A, Chaikelson J. 1995. Structural equation model of intellectual change and continuity and predictors of intelligence in older men. Psychol Aging. 10:294–303.

Grober E, Sliwinski M. 1991. Development and validation of a model for estimating premorbid verbal intelligence in the elderly. J Clin Exp Neuropsychol. 13:933–949.

Habeck C, Hilton HJ, Zarahn E, Flynn J, Moeller JR, Stern Y. 2003. Relation of cognitive reserve and task performance to expression of regional covariance networks in an event-related fMRI study of nonverbal memory. Neuroimage. 20:1723–1733.

Habeck C, Rakitin BC, Moeller J, Scarmeas N, Zarahn E, Brown T, Stern Y. 2005. An event-related fMRI study of the neural networks underlying the encoding, maintenance, and retrieval phase in a delayed-match-to-sample task. Brain Res Cogn Brain Res. 23(2–3):207–220.

Holmes A, Friston K. 1998. Generalisability, random effects and population inference. Neuroimage. 7:S754.

Holtzer R, Stern Y, Rakitin BC. 2004. Age-related differences in executive control of working memory. Mem Cogn. 32(8):1333–1345.

Hultsch DF, Hertzog C, Small GW, Dixon RA. 1999. Use it or lose it: engaged lifestyle as a buffer of cognitive decline in aging? Psychol Aging. 14:245–263.

Kwong KK, Beliveau JW, Chesler DA, Goldberg IE, Weisskoff RM, Poncelet BP, Kennedy DN, Hoppel BE, Cohen MS, Turner R, et al. 1992. Dynamic magnetic resonance imaging of human brain activity during primary sensory stimulation. Proc Natl Acad Sci USA. 89: 5675–5679.

Lancaster JL, Woldorff MG, Parsons LM, Liotti M, Freitas CS, Rainey L, Kochunov PV, Nickerson D, Mikiten SA, Fox PT. 2000. Automated Talairach Atlas labels for functional brain mapping. Hum Brain Mapp. 10:120–131.

Manly JJ, Touradji P, Tang M-X, Stern Y. 2003. Literacy and memory decline among ethnically diverse elders. J Clin Exp Neuropsychol. 5:680–690.

Mattis S, Bellak L, Karasu TB. 1976. Mental status examination for organic mental syndrome in the elderly patient. In: Geriatric psychiatry. New York (NY): Grune & Stratton. p. 77–121.

Ogawa S, Menon RS, Tank DW, Kim SG, Merkle H, Ellermann JM, Ugurbil K. 1993. Functional brain mapping by blood oxygenation level-dependent contrast magnetic resonance imaging. A comparison of signal characteristics with a biophysical model. Biophys J. 64:803–812.

Richards M, Sacker A. 2003. Lifetime antecedents of cognitive reserve. J Clin Exp Neuropsychol. 25(5):614–624.

Scarmeas N, Levy G, Tang MX, Manly J, Stern Y. 2001. Influence of leisure activity on the incidence of Alzheimer's disease. Neurology. 57(12): 2236–2242.

Scarmeas N, Zarahn E, Anderson KE, Hilton HJ, Flynn J, Van Heertum RL, Sackeim HA, Stern Y. 2003. Cognitive reserve and non-verbal memory associated PET brain activation in young and healthy elderly. Neuroimage. 19:1215–1227.

Schaie KW. 1984. Midlife influences upon intellectual functioning in old age. Int J Behav Dev. 7:463–478.

Snodgrass JG, Corwin J. 1998. Pragmatics of measuring recognition memory: application to dementia and amnesia. J Exp Psychol Gen. 117:34–50.

Stern Y. 2002. What is cognitive reserve? Theory and research application of the reserve concept. J Int Neuropsychol Soc. 8:448–460.

Stern Y, Gurland B, Tatemichi TK, Tang MX, Wilder D, Mayeux R. 1994. Influence of education and occupation on the incidence of Alzheimer's disease. JAMA. 271:1004–1010.

Stern Y, Habeck C, Moeller J, Scarmeas N, Anderson KE, Hilton HJ, Flynn J, Sackeim H, Van Heertum R. 2005. Brain networks associated with cognitive reserve in healthy young and old adults. Cereb Cortex. 15(4):394–402.

Stern Y, Sano M, Paulson J, Mayeux R. 1987. Modified mini-mental state examination: Validity and reliability. Neurology. 37(Suppl 1):179.

Stern Y, Zarahn E, Hilton HJ, Delapaz R, Flynn J, Rakitin B. 2003. Exploring the neural basis of cognitive reserve. J Clin Exp Neuropsychol. 5:691–701.

Sternberg S. 1966. High-speed scanning in human memory. Science. 153:652.

Talairach JTP. 1988. Co-planar stereotaxic atlas of the human brain: an approach to medical cerebral imaging. Stuttgart, New York: Thieme Medical Publishers, Inc.

Wager TD, Jonides J, Reading S. 2003. Neuroimaging of shifting attention: a meta-analysis. Neuroimage. 22:1679–1693.

Wager TD, Smith EE. 2006. Neuroimaging studies of working memory: a meta-analysis. Cogn Affect Behav Neurosci. 3:255–274.

Wechsler D. 1981. Wechsler adult intelligence scale-revised. New York (NY): The Psychological Corporation.

Wilson RS, Bennett DA, Gilley DW, Beckett LA, Barnes LL, Evans DA. 2000. Premorbid reading activity and patterns of cognitive decline in Alzheimer disease. Arch Neurol. 57(12):1718–1723.

Wilson RS, Mendes De Leon CF, Barnes LL, Schneider JA, Bienias JL, Evans DA, Bennett DA. 2002. Participation in cognitively stimulating activities and risk of incident Alzheimer disease. JAMA. 287(6): 742–748.

Worsley KJ. 1994. Local maxima and the expected Euler characteristic of excursion sets of chi-squared, f and t fields. Adv Appl Probab. 26:13–42.

Worsley KJ, Poline JB, Friston KJ, Evans AC. 1997. Characterizing the response of PET and fMRI data using multivariate linear models. Neuroimage. 6(4):305–319.

Zarahn E, Rakitin B, Abela D, Flynn J, Stern Y. 2005. Positive evidence against human hippocampal involvement in working memory maintenance of familiar stimuli. Cereb Cortex. 15:303–316.

Zarahn E. 2000. Testing for neural responses during temporal components of trials with BOLD fMRI. Neuroimage. 11:783–796.